Mineralogical Magazine (2025), **89**, 566–574
doi:10.1180/mgm.2025.9

CAMBRIDGE UNIVERSITY PRESS

Article

The synthetic analogue of kotulskite and its solid-solution series with selected elements

Anna Vymazalová[1], František Laufek[1], Jan Kamenský[1,2] and Marek Tuhý[1,2]

[1]Czech Geological Survey, Geologická 6, 152 00, Prague 5, Czech Republic and [2]Institute of Geochemistry, Mineralogy and Mineral Resources, Faculty of Science, Charles University, Albertov 6, 128 43, Prague 2, Czech Republic

Abstract

The solubility of Ag, As, Bi, Cu, Pb, Sb and Sn in the synthetic analogue of kotulskite (PdTe) was studied experimentally at 400°C (for Bi at 500°C). The extent of the solid solution was studied on the line PdTe–PdA with a compositional range $Pd(Te_{1-x}A_x)$ with $x = 0.1, 0.2, 0.4$ and 0.6 and A = Ag, As, Bi, Cu, Pb, Sb and Sn. For the purpose of this study the silica-glass tube method was used. The experimental products were evaluated by means of powder X-ray diffraction analysis, reflected light and electron microscopy. Kotulskite does not dissolve Ag. It may dissolve up 3 at.% As, up to 5.6 at.% Cu, up to 20 at.% Sn and up to 30 at.% Pb. A complete solid solution between kotulskite (PdTe) – sudburyite (PdSb) and kotulskite (PdTe) – sobolevskite (PdBi) as suggest from natural occurrences has not been confirmed within this study. There is a composition gap between $Pd_{0.99}(Te_{0.21}Bi_{0.80})_{\Sigma 1.01}$ (PdTe dissolving 40.3 at.% Bi) and $Pd_{1.00}(Bi_{0.97}Te_{0.03})_{\Sigma 1.00}$ (PdBi dissolving 1.6 at.% Te). Also, there seems to be a gap between $Pd_{1.00}(Te_{0.18}Sb_{0.82})_{\Sigma 1.00}$ (PdTe dissolving 41.1 at.% Sb) and PdSb. The Cu substitutes for Pd whereas As, Bi, Pb, Sb and Sn substitute for Te in the crystal structure of kotulskite. Assessed solid solution series should be sought in assemblages with other platinum-group minerals and known Pd tellurides, likely in magmatic Cu–Ni–PGE mineral deposits, associated with mafic and ultramafic igneous rocks.

Keywords: kotulskite; PdTe; platinum-group mineral; solid solution; experimental study

(Received 2 December 2024; accepted 24 January 2024; Accepted Manuscript published online: 31 January 2025)

Introduction

There are four known palladium telluride minerals: kotulskite (PdTe), merenskyite ($PdTe_2$), telluropalladinite (Pd_9Te_4) and keithconnite ($Pd_{3-x}Te$). There are also known occurrences of minerals with possible compositions of $Pd_{13}Te_3$ and Pd_3Te_2 (e.g. Arnason *et al.*, 1997). However, these minerals have not yet been fully characterised. Among palladium tellurides, kotulskite (Genkin *et al.*, 1963) and merenskyite (Kingston, 1966) belong to the most abundant platinum group minerals, commonly found together with other platinum-group minerals and Cu–Ni–Fe sulfides. Palladium tellurides are generally found in Cu–Ni–PGE mineral deposits, associated with mafic and ultramafic igneous rocks. They also occur in other types of deposits, enriched in PGE, like porphyry copper/gold systems, sedimentary hosted massive sulfides or metalliferous black shales.

In nature, kotulskite rarely occurs as a purely PdTe phase. It commonly contains an admixture of other elements. Probably the most common is the substitution of Pt for Pd and Bi for Te. The solubility of Bi is well established and some literature data suggest there is almost a complete solid solution between kotulskite (PdTe) and sobolevskite (PdBi), e.g. Cabri (2002, pp 59–61) and Evstigneeva *et al.* (1976). However, in most cases, this is only supported by electron probe micro-analyses (EPMA) or scanning electron microscopy (SEM) data; no further XRD data or structural data are available. A compositional set of Bi solubility in kotulskite from various ore deposits is summarised in Table 1 and plotted in Fig. 1. The solubility of other selected elements in kotulskite in nature is also summarised in Table 1. Kotulskite can dissolve As (0.42 wt.%, Noril'sk deposits, Russia, Tolstykh *et al.*, 2019). It also dissolves Cu (0.98 wt.%, Burakovsk complex, Russia, Grokhovskaya *et al.*, 2005). Kotulskite with Pb (up to 14 wt.%) has been observed from various localities worldwide such as the Noril'sk deposits (Kovalenker *et al.*, 1973, Sluzhenikin, 2011); Burakovsk complex (Grokhovskaya *et al.*, 2005); Kondyor complex (Barkov *et al.*, 2017); Yoko–Dovyren intrusion in Russia (Spiridonov *et al.*, 2019); Two Duck Lake intrusion in Canada (Watkinson and Ohnenstetter, 1992); and the Stillwater Complex, Montana, USA (Cabri *et al.*, 1979). It commonly dissolves Sb, suggesting the formation of a complete solid solution between kotulskite and sudburyite (PdSb), e.g. Evstigneeva *et al.* (1976), Cabri (2002, pp 59–61).

In order to define the range of substitution in kotulskite we have experimentally investigated the solubility of selected elements (Ag, As, Bi, Cu, Pb, Sb and Sn) in the synthetic analogue of kotulskite at 400°C. At this temperature the equilibrium is attained in sufficient time (in months), and is close to the post magmatic conditions for formation of such assemblages in nature. At higher temperatures the reactions would be faster due to better kinetics and the

Corresponding author: Anna Vymazalová; Email: anna.vymazalova@geology.cz
Associate Editor: David Hibbs
Cite this article: Vymazalová A., Laufek F., Kamenský J. and Tuhý M. (2025) The synthetic analogue of kotulskite and its solid-solution series with selected elements. *Mineralogical Magazine* **89**, 566–574. https://doi.org/10.1180/mgm.2025.9

© The Author(s), 2025. Published by Cambridge University Press on behalf of The Mineralogical Society of the United Kingdom and Ireland.

https://doi.org/10.1180/mgm.2025.9 Published online by Cambridge University Press

Table 1. Solubility of As, Bi, Cu, Sb and Pb in kotulskite from various occurrences reported in literature.

Element	Content in PdTe (wt.%)	Occurrence	Reference
As	0.36 to 0.42	Noril'sk deposits, Russia	Tolstykh *et al.* (2019)
Bi	1.2 to 2.6	Stillwater Complex, Montana, USA	Cabri *et al.* (1979)
	1.5 to 9.2	Lac des Iles, Ontario, Canada	Cabri and Laflamme (1979)
	9.56 to 10.19	Retty Lake, Quebec, Canada	Beaudoin *et al.* (1990)
	12.54 to 14.55	Noril'sk deposits, Russia	Tolstykh *et al.* (2019)
	1.12 to 16.75	Yoko-Dovyren intrusion, Russia	Spiridonov *et al.* (2019)
	17.9	Bleïda Far West, Anti-Atlas, Morocco	El Ghorfi *et al.* (2006)
	24.22	Monchegorsk complex, Russia	Konnikov *et al.* (1993)
	up to 27.1	Wellgreen deposit, Yukon, Canada	Barkov *et al.* (2002)
	17.94 to 27.13	Lukkulaisvaara intrusion, Russia	Grokhovskaya *et al.* (1992)
	23.71 to 28.25	Oktyabrsky mine, Noril'sk, Russia	Spiridonov *et al.* (2020)
	12.01 to 28.76	Kaalamo massif, Russia	Lavrov and Kuleshevich (2017)
	29.22	Monchepluton, Russia	Barkov *et al.* (2022)
	18.3 to 30.6	Rustenburg mine, Bushveld, JAR	Kingston (1966)
	21.3 to 30.9	Oktyabrsky mine, Noril'sk, Russia	Kovalenker *et al.* (1973)
	27.87 to 31.64	Blue Lake, Quebec, Canada	Beaudoin *et al.* (1990)
	19.58 to 32.23	Two Duck Lake intrusion, Canada	Watkinson and Ohnenstetter (1992)
	31.29 to 33.28	Sudbury, Ontario, Canada	Cabri *et al.* (1996)
	33.57	Chineisky layered intrusion, Russia	Tolstykh (2008)
	33.2 to 35.3	Sudbury, Ontario, Canada	Cabri and Laflamme (1976)
	6.14 to 36.02	Geordie Lake intrusion, Coldwell Complex, Canada	Mulja and Mitchell (1991)
	34.64 to 39.69	Burakovsk layered complex, Russia	Grokhovskaya *et al.* (2005)
	49.0	Noril'sk deposits, Russia	Yushko-Zakharova *et al.* (1972)
	series PdTe-PdBi	Oktyabrsky mine, Noril'sk, Russia	Evstigneeva *et al.* (1976)
	series PdTe-PdBi	Oktyabrsky mine, Noril'sk, Russia	Barkov *et al.* (2021)
Cu	0.98	Burakovsk layered complex, Russia	Grokhovskaya *et al.* (2005)
Ni	0.05	Sudbury, Ontario, Canada	Cabri and Laflamme (1976)
	0.1	Merensky Reef, Bushveld, JAR	Criddle and Stanley (1993)
Sb	13.49 to 17.27	Savabeisky ore occurrence, Russia	Shaybekov *et al.* (2021)
	series PdTe-PdSb	Oktyabrsky mine, Noril'sk, Russia	Evstigneeva *et al.* (1976)
Pb	3.87	Burakovsk layered complex, Russia	Grokhovskaya *et al.* (2005)
	7.93 to 9.55	Two Duck Lake intrusion, Canada	Watkinson and Ohnenstetter (1992)
	11.0 to 13.54	Yoko-Dovyren intrusion, Russia	Spiridonov *et al.* (2019)

solubility would probably increase. However, in most cases within the systems studied, a liquid phase appears. Therefore, only the solubility of Bi in kotulskite was studied additionally at 500°C.

Further, we determined the extent of the kotulskite solid solution and characterised it in terms of unit-cell parameters and volume. We also tentatively explored the stable association of kotulskite solid solution (ss) in the corresponding ternary systems. A comparison of experimental results with natural occurrences is briefly discussed. In nature, kotulskite often incorporates more than one element such as Pd(Te,Bi,Sb) (e.g. Beaudoin *et al.*, 1990; Cabri and Laflamme, 1976; Tolstykh, 2008) or Pd(Te,Bi,Pb) (e.g. Evstigneeva *et al.*, 1976; Spiridonov *et al.*, 2019). However, experimentally it is difficult to attain equilibrium within a multicomponent system so in this study we deal with one element solubility. The incorporation of additional elements will be a matter of further studies.

Methods and techniques

Experimental

The silica-glass tube method was used for this study. Charges of ~300–400 mg were carefully weighed out from the native elements (palladium powder, 99.95% purity; tellurium ingot, 99.999% purity; and selected elements Ag, As, Bi, Cu, Pb, Sb and Sn of 99.999% purity). Then, the silica-glass tubes with charges were sealed under vacuum and the starting mixtures were melted at 1000°C for several hours. The run products were ground in an agate mortar using acetone and reheated at 400°C (for 3 to 4 months), additionally at 500°C for the Pd–Te–Bi system, and some other attempts with Sb and Sn were made. After heating, samples were quenched by dropping the capsules in cold water. The run products were studied initially using powder X-ray diffraction, and polished sections were examined under reflected light and subsequently analysed using EPMA.

We performed the experimental runs in Pd–Te–A systems, where A = Ag, As, Bi, Cu, Pb, Sb or Sn; with a compositional step from 5 to 10 at.%. The experimental runs were studied on the line PdTe–PdA with a compositional range $Pd_{50}(Te_{50-x}A_x)$ with $x = 5$, 10, 20 and 30. In addition, the solubility of Bi and Sb were studied in a detail for the range with $x = 5$, 10, 20, 30, 35, 40, 45 and 50. Some additional runs were also performed towards the line PdTe–ATe within the range $(Pd_{50-x}A_x)Te_{50}$, with $x = 10$ and 20. The list of experiments conducted is given in Table 2.

X-ray diffraction analyses

The X-ray diffraction patterns (XRD) were collected in Bragg–Brentano geometry on a Bruker D8 Advance diffractometer

https://doi.org/10.1180/mgm.2025.9 Published online by Cambridge University Press

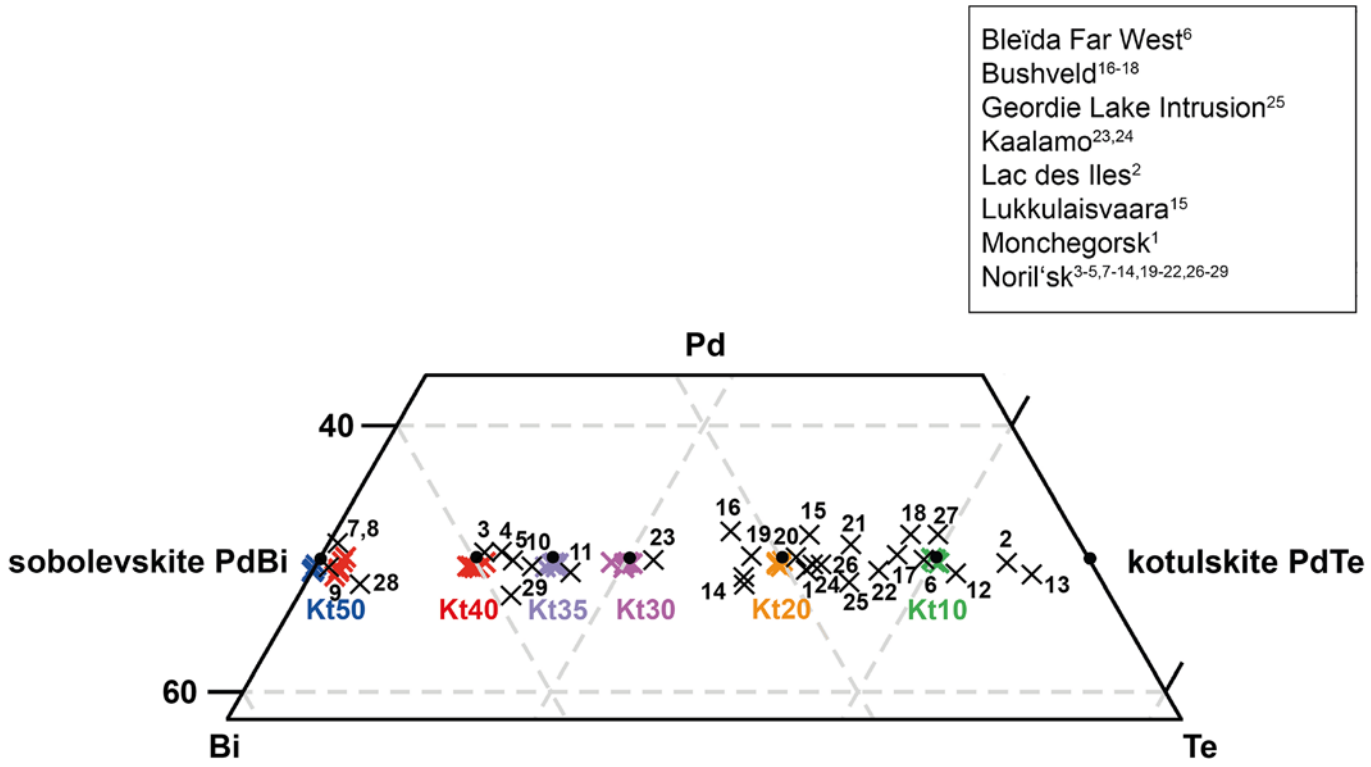


Figure 1. A plot (in at.%) of kotulskite dissolving Bi from various localities. Black dots show starting composition of experiments performed, in colour are given EPMA data. References: [1]Barkov *et al.* (2022); [2]Cabri and Laflamme (1979); [3–5]Cook *et al.* (2002); [6]El Ghorfi *et al.* (2006); [7–14]Evstigneeva *et al.* (1976); [15]Grokhovskaya *et al.* (1992); [16–18]Kingston (1966); [19–22]Kovalenker *et al.* (1973); [23,24]Lavrov and Kuleshevich (2017); [25]Mulja and Mitchell (1991); [26]Spiridonov *et al.* (2020); [27]Tolstykh *et al.* (2019); and [28,29]Yushko–Zakharova *et al.* (1972).

Table 2. A list of experiments performed.

	Starting composition (at.%)				Starting composition (at.%)		
Run No.	Pd	Te	A	Run No.	Pd	Te	A
A = Ag				X = Cu			
KtAg10	50	40	10	KtCu0.5	50	45	5
AgPdTe1	40	50	10	KtCu10	50	40	10
AgPdTe2	30	50	20	KtCu20	50	30	20
A = As				KtCu30	50	20	30
KtAs0.5	50	45	5	X = Pb			
KtAs10	50	40	10	KtPb0.5	50	45	5
KtAs20	50	30	20	KtPb10	50	40	10
KtAs30	50	20	30	KtPb20	50	30	20
AsPdTe1	40	50	10	KtPb30	50	20	30
AsPdTe2	30	50	20	X = Sb			
A = Bi				KtSb0.5	50	45	5
KtBi0.5	50	45	5	KtSb10	50	40	10
KtBi10	50	40	10	KtSb20	50	30	20
KtBi20	50	30	20	KtSb30	50	20	30
KtBi30	50	20	30	KtSb40	50	10	40
KtBi35	50	15	35	KtSb45	50	5	45
KtBi40	50	10	40	KtSb50	50	0	50
KtBi43	50	7	43	SbPdTe1	40	50	10
KtBi45	50	5	45	SbPdTe2	30	50	20
KtBi47	50	3	47	KtSb43	50	7	43
KtBi50	50	0	50	KtSb47	50	3	47
BiPdTe1	40	50	10	X = Sn	50	40	10
BiPdTe2	30	50	20	KtSn0.5	50	45	5
A = Cu				KtSn10	50	40	10
CuPdTe1	40	50	10	KtSn20	50	30	20
CuPdTe2	30	50	20	KtSn30	50	20	30

https://doi.org/10.1180/mgm.2025.9 Published online by Cambridge University Press

Table 3. Phase assemblages in the experimental runs and the composition of kotulskite solid-solution series, based on XRD and EPMA data (A = As, Bi, Cu, Pb, Sb or Sn).

Run No.	Phase assemblage at 400°C (*500°C)	Kotulskite ss	A in PdTe (at.%)
KtAg10		$Pd_{1.00}Te_{1.00}$	0
AgPdTe1		$Pd_{1.00}Te_{1.00}$	0
As			
KtAs0.5	$Pd(Te,As)_{ss}$ + $Pd(As,Te)_{2\ ss}$	$Pd_{0.96}(Te_{1.01}As_{0.03})_{\Sigma 1.04}$	1.8
KtAs10	$Pd(Te,As)_{ss}$ + $Pd(As,Te)_{2\ ss}$ + Pd_2As	$Pd_{0.95}(Te_{1.00}As_{0.05})_{\Sigma 1.05}$	2.8
KtAs20	$Pd(Te,As)_{ss}$ + $Pd(As,Te)_{2\ ss}$ + Pd_2As	$Pd_{0.95}(Te_{1.00}As_{0.05})_{\Sigma 1.05}$	2.8
KtAs30	$Pd(Te,As)_{ss}$ + $Pd(As,Te)_{2\ ss}$ + Pd_2As	$Pd_{0.95}(Te_{1.02}As_{0.07})_{\Sigma 1.09}$	3.0
AsPdTe1	$Pd(Te,As)_{ss}$ + $Pd(As,Te)_{2\ ss}$ + $PdTe_2$	$Pd_{0.94}(Te_{1.01}As_{0.05})_{\Sigma 1.06}$	2.7
AsPdTe2	$PdAs_2$ + $PdTe_{2\ ss}$ + As_2Te_3		—
Bi*			
KtBi0.5	$Pd(Te,Bi)_{ss}$	$Pd_{1.00}(Te_{0.91}Bi_{0.09})_{\Sigma 1.00}$	4.7
KtBi10	$Pd(Te,Bi)_{ss}$	$Pd_{1.00}(Te_{0.80}Bi_{0.20})_{\Sigma 1.00}$	10.1
KtBi20	$Pd(Te,Bi)_{ss}$	$Pd_{1.00}(Te_{0.60}Bi_{0.40})_{\Sigma 1.00}$	20.3
KtBi30	$Pd(Te,Bi)_{ss}$	$Pd_{0.99}(Te_{0.40}Bi_{0.61})_{\Sigma 1.01}$	30.4
KtBi35	$Pd(Te,Bi)_{ss}$	$Pd_{0.99}(Te_{0.31}Bi_{0.70})_{\Sigma 1.01}$	35.1
KtBi40	$Pd(Te,Bi)_{ss}$ + $Pd(Bi,Te)_{ss}$ **	$Pd_{0.99}(Te_{0.21}Bi_{0.80})_{\Sigma 1.01}$	40.2
KtBi45	$Pd(Te,Bi)_{ss}$ + $Pd(Bi,Te)_{ss}$ **	$Pd_{0.99}(Te_{0.21}Bi_{0.80})_{\Sigma 1.01}$	40.2
KtBi50	PdBi (monoclinic)		—
BiPdTe1	$Pd_{0.89}Te_{0.90}Bi_{0.21}$ + $PdTe_{2\ ss}$		11.0
BiPdTe1	$PdTe_2$ ss + ?		—
Cu			
KtCu0.5	$(Pd,Cu)Te_{ss}$ + $Pd_3Te_{2\ ss}$? + Cu-telluride ss	$(Pd_{0.98}Cu_{0.01})_{\Sigma 0.99}Te_{1.01}$	0.7
KtCu10	$(Pd,Cu)Te_{ss}$ + $Pd_3Te_{2\ ss}$ + Cu-telluride ss	$(Pd_{0.98}Cu_{0.01})_{\Sigma 0.99}Te_{1.01}$	0.9
KtCu20	$Pd_9Te_{4\ ss}$ + $Pd_3Te_{2\ ss}$+ $PdCu_3$		—
KtCu30	PdCu + $PdCu_3$ + $Pd_{20}Te_{7\ ss}$		—
CuPdTe1	$(Pd,Cu)Te_{\ ss}$ + Cu-telluride ss	$(Pd_{0.91}Cu_{0.05})_{\Sigma 0.96}Te_{1.04}$	3.1
CuPdTe2	$(Pd,Cu)Te_{\ ss}$ + $PdTe_2$ + Cu-telluride ss	$(Pd_{0.85}Cu_{0.09})_{\Sigma 0.94}Te_{1.06}$	5.6
Pb			
KtPb0.5	$Pd(Te,Pb)_{ss}$	$Pd_{1.01}(Te_{0.92}Pb_{0.07})_{\Sigma 0.99}$	5.8
KtPb10	$Pd(Te,Pb)_{ss}$	$Pd_{1.01}(Te_{0.83}Pb_{0.16})_{\Sigma 0.99}$	11.8
KtPb20	$Pd(Te,Pb)_{ss}$	$Pd_{1.01}(Te_{0.59}Pb_{0.40})_{\Sigma 0.99}$	21.3
KtPb30	$Pd(Te,Pb)_{ss}$ + $Pb_{13}Pb_9$ + PbTe	$Pd_{1.00}(Te_{0.40}Pb_{0.61})_{\Sigma 1.01}$	30.3
Sb			
KtSb0.5	$Pd(Te,Sb)_{ss}$ + Pd_8Sb_3	$Pd_{0.98}(Te_{0.93}Sb_{0.09})_{\Sigma 1.02}$	4.7
KtSb10	$Pd(Te,Sb)_{ss}$ + Pd_8Sb_3	$Pd_{0.97}(Te_{0.84}Sb_{0.19})_{\Sigma 1.03}$	9.6
KtSb20	$Pd(Te,Sb)_{ss}$ + Pd_8Sb_3	$Pd_{0.98}(Te_{0.63}Sb_{0.39})_{\Sigma 1.02}$	19.8
KtSb30	$Pd(Te,Sb)_{ss}$ + Pd_8Sb_3	$Pd_{1.00}(Te_{0.39}Sb_{0.61})_{\Sigma 1.00}$	30.5
KtSb35	$Pd(Te,Sb)_{ss}$	$Pd_{1.00}(Te_{0.30}Sb_{0.70})_{\Sigma 1.00}$	35.1
KtSb40	$Pd(Te,Sb)_{ss}$	$Pd_{1.00}(Te_{0.18}Sb_{0.82})_{\Sigma 1.00}$	41.1
KtSb45	$Pd(Te,Sb)_{ss}$? + xx ?		—
KtSb50	PdSb	$Pd_{1.01}Sb_{0.90}$	49.4
Sn			
KtSn0.5	$Pd(Te,Sn)_{ss}$	$Pd_{1.01}(Te_{0.90}Sn_{0.09})_{\Sigma 0.99}$	5.0
KtSn10	$Pd(Te,Sn)_{ss}$ + Pd_2Sn	$Pd_{0.97}(Te_{0.83}Sn_{0.20})_{\Sigma 1.03}$	9.8
KtSn20	$Pd(Te,Sn)_{ss}$ + Pd_2Sn	$Pd_{0.93}(Te_{0.74}Sn_{0.32})_{\Sigma 1.06}$	16.5
KtSn30	$Pd(Te,Sn)_{ss}$ + $Pd_{20}Sn_{13}$? + PdSnTe	$Pd_{0.93}(Te_{0.63}Sn_{0.44})_{\Sigma 1.07}$	20.6

**monoclinic PdBi (dissolving 1.6 at.% Te), ss - solid solution

equipped with the Lynx Eye XE detector and Cu*K*α radiation source. The data were collected in the angular range from 10 to 140°2θ with step size of 0.015°2θ and 1.2 second counting time per step. Qualitative phase analysis of samples was performed using the *HighScore* program 3.0c (PANalytical, 2012) and the PDF-2018 database. A subsequent Rietveld refinement, carried out by *Topas 5* (Bruker AXS, 2014), was used for calculation of unit-cell parameters of the kotulskite solid-solution series. The crystal structure data of Gronvold and Rost (1956) for synthetic PdTe were used in our refinements. Crystal structure models of other minor phases detected in our experiments were adopted from the Inorganic Crystal Structure Database (Zagorac *et al.*, 2019). In general, the Rietveld refinements involved refinement of scale factors, unit-cell parameters, and isotropic size and isotropic strain parameters. As all atoms in the kotulskite structure are in special positions, there are no structural parameters to refine. The background was determined employing a Chebyshev polynomial function of the 6th order.

https://doi.org/10.1180/mgm.2025.9 Published online by Cambridge University Press

Table 4. The unit-cell parameters of the kotulskite solid-solution series.

Run No.	Content of A	Unit-cell parameters		
	(at.%)	*a* [Å]	*c* [Å]	*V* [Å^3]
PdTe	0	4.1523(1)	5.6719(2)	84.69(1)
A = As				
KtAs0.5	1.8	4.1215(1)	5.6474(2)	83.08(1)
KtAs10	2.8	4.1147(1)	5.6431(2)	82.74(1)
A = Bi*				
KtBi0.5	4.7	4.1607(1)	5.6696(2)	85.00(1)
KtBi10	10.2	4.1685(1)	5.6688(2)	85.30(1)
KtBi20	20.5	4.1851(1)	5.6755(2)	86.08(1)
KtBi30	30.6	4.1962(1)	5.6836(2)	86.66(1)
KtBi35	35.7	4.2036(1)	5.6899(2)	87.07(1)
KtBi40	40.7	4.2074(1)	5.6942(2)	87.29(1)
KtBi45	40.7	4.2082(1)	5.6942(2)	87.33(1)
A = Cu				
KtCu0.5	0.7	4.1527(1)	5.6676(2)	84.64(1)
CuPdTe1	3.1	4.1531(1)	5.6234(2)	83.99(1)
CuPdTe2	5.6	4.1479(1)	5.6051(2)	83.51(1)
A = Pb				
KtPb05	5.8	4.1540(1)	5.6726(2)	84.77(1)
KtPb10	11.8	4.1553(1)	5.6772(2)	84.89(1)
KtPb20	21.3	4.1555(1)	5.6897(2)	85.08(1)
KtPb30	30.3	4.1469(1)	5.7003(2)	84.89(1)
A = Sb				
KtSb0.5	4.7	4.1405(1)	5.6544(2)	83.95(1)
KtSb10	9.6	4.1336(1)	5.6430(2)	83.50(1)
KtSb20	19.8	4.1210(1)	5.6252(2)	82.73(2)
KtSb30	30.5	4.1098(1)	5.6139(2)	82.11(2)
KtSb35	35.1	4.1045(1)	5.6098(2)	81.84(1)
KtSb40	41.1	4.9066(1)	5.6042(2)	81.45(1)
KtSb50	49.4	4.0768(1)	5.5928(2)	80.50(1)
A = Sn				
KtSn0.5	4.5	4.1523(1)	5.6719(2)	84.69(1)
KtSn10	9.9	4.1187(1)	5.6367(2)	82.80(1)
KtSn20	16.2	4.0800(1)	5.5865(2)	84.54(1)
KtSn30	20.1	4.0608(1)	5.5800(2)	79.99(1)

*500°C

Electron-probe microanalyses

The EPMA analyses were performed with a JEOL JXA 8230 electron probe microanalyser in wavelength-dispersion mode using an electron beam focussed to 1–2 μm. Pure elements were used as standards. Concentrations were quantified on the *L*α lines for Pd, Te, As, Sb, Se, Sn, Pb; *L*β for Ag; *K*α for Cu and *M*α for Bi; with an accelerating voltage of 15 keV, and a beam current of 10 nA. Compositional data were collected from several grains within a polished section of the sample.

Results and discussion

The list of experimental runs performed is summarised in Table 2. Phase assemblages observed in the experimental products and the composition of kotulskite solid-solution series samples are given in Table 3. The unit-cell parameters of kotulskite solid-solution samples are summarised in Table 4, and the change of unit-cell volume is plotted in Fig. 2. Selected experimental run products with kotulskite ss are shown in Fig. 3.

Silver solubility

Kotulskite does not dissolve Ag at 400°C which is in agreement with the experimental study of the system Ag–Pd–Te at 350 and 450°C (Vymazalová *et al.*, 2015).

Arsenic solubility

The ternary system As–Pd–Te was studied by El-Boragy and Schubert (1971) at 480°C. According to their phase diagram PdTe dissolves up to 20 at.% As at 480°C, however more detail data are not available. Our experimental study has shown the maximum solubility of As in kotulskite up to 3 at.% at 400°C. Kotulskite ss forms a stable association with palladoarsenide (Pd_2As) and phase $PdAs_2$ at 400°C (Fig. 3a,b). It also coexists with $PdAs_2$ and merenskyite ($PdTe_2$).

Minute incorporation of As (up to 0.05 apfu) results in a decrease of the unit-cell volume from 84.69 to 82.74 Å^3.

Bismuth solubility

The system Pd–Bi–Te has been preliminarily studied by Evstigneeva *et al.* (2019) in the temperature range 350–550°C.

https://doi.org/10.1180/mgm.2025.9 Published online by Cambridge University Press

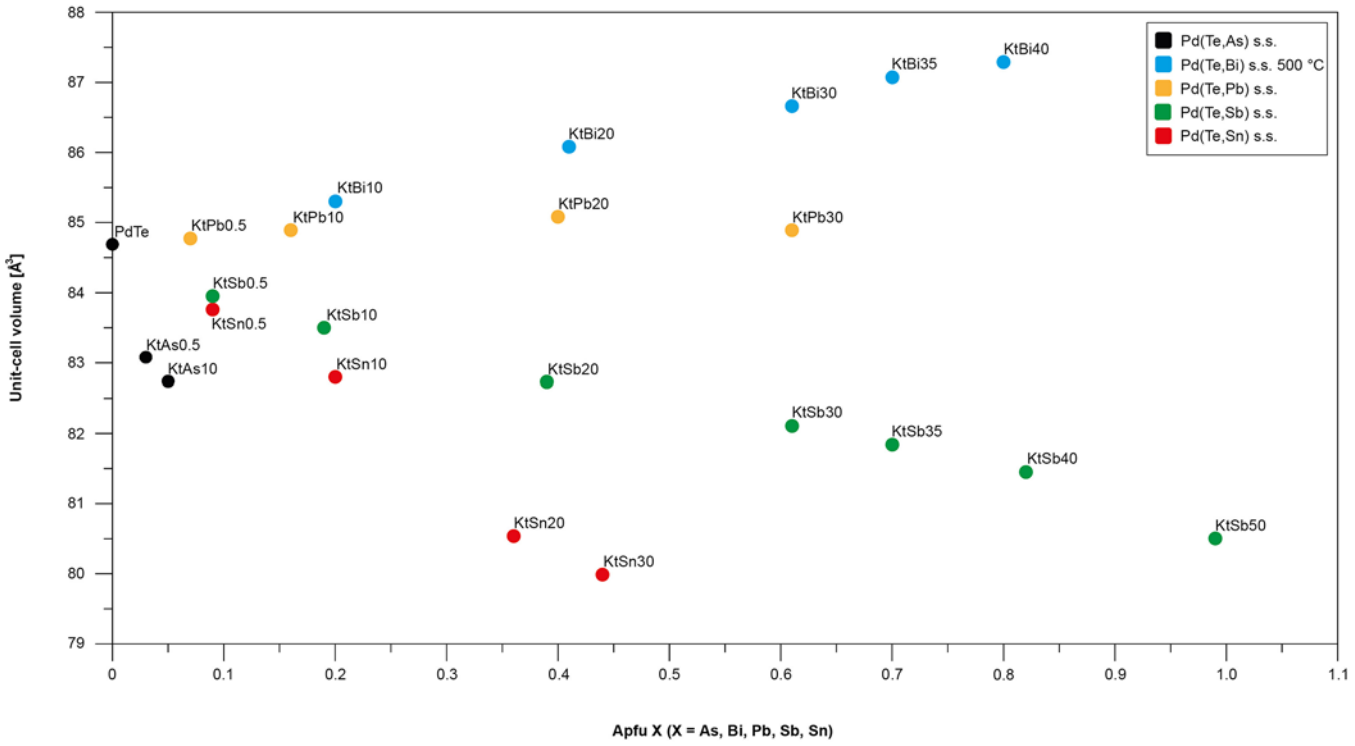


Figure 2. The unit-cell volume of kotulskite solid solutions.

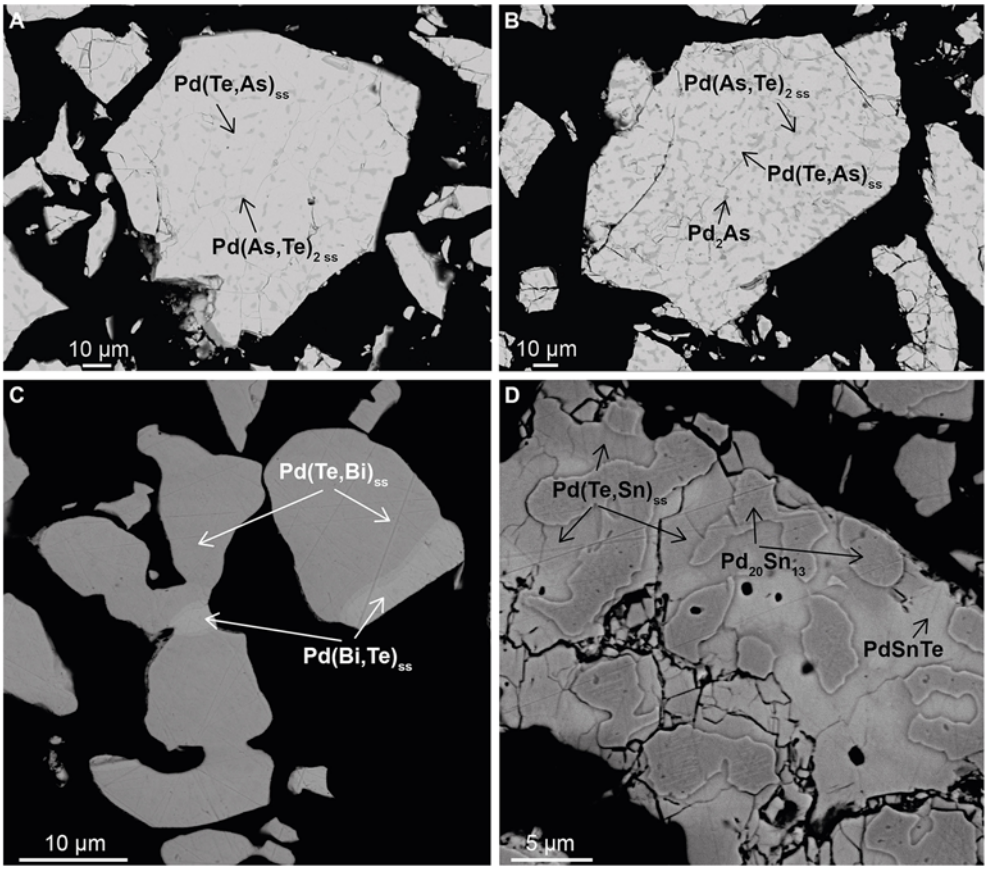


Figure 3. Back-scattered electron images of synthetic analogue of kotulskite: (a) PdTe dissolving 1.8 at.% As ($Pd_{0.96}(Te_{1.01}As_{0.03})_{\Sigma 1.04}$) in association with $Pd(As,Te)_2$ ss; (b) PdTe dissolving 2.8 at.% As ($Pd_{0.95}(Te_{1.00}As_{0.05})_{\Sigma 1.05}$) in association with $Pd(As,Te)_2$ ss and Pd_2As; (c) PdTe dissolving 40.2 at.% Bi ($Pd_{0.99}(Te_{0.21}Bi_{0.80})_{\Sigma 1.01}$) in association with PdBi dissolving 1.6 at.% Te; (d) Sn-rich PdTe dissolving 20.1 at.% Sn ($Pd_{0.93}(Te_{0.63}Sn_{0.44})_{\Sigma 1.07}$) in association with $Pd_{20}Sn_{13}$ and PdSnTe phases.

https://doi.org/10.1180/mgm.2025.9 Published online by Cambridge University Press

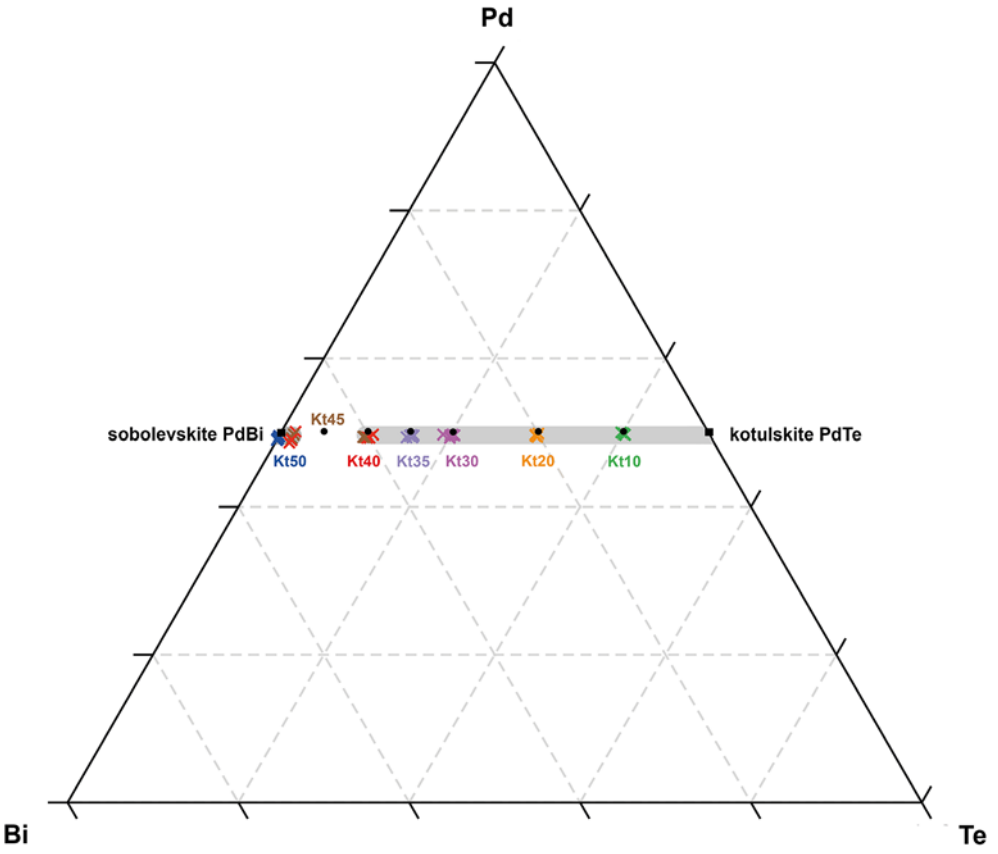


Figure 4. A plot showing a compositional gap in a solid-solution series PdTe–PdBi in the ternary diagram at 500°C. Black dots show the starting composition of experiments, in colour are given EPMA data (see Tables 2 and 3).

Their results suggest a limited solubility of Bi in kotulskite. Kotulskite–sobolevskite-series minerals have been widely reported from a number of Cu–Ni–PGE mineral deposits associated with mafic and ultramafic igneous rocks (e.g. Evstigneeva *et al.*, 1976; Cabri, 2002; Cook *et al.*, 2002; Barkov *et al.*, 2021; among others). Figure 1 shows the solubility of Bi in kotulskite from various natural occurrences.

At 400°C the Bi-rich experimental products display a certain degree of inhomogeneity therefore the experiments were further heated at 500°C for 1 month. This inhomogeneity was evident in the powder X-ray diffraction patterns of experimental runs KtBi30, KtBi35 and KtBi40 (Table 2), which showed apparent broad and asymmetric peaks. These diffraction patterns could not be fitted in the Rietveld refinement by a single hexagonal kotulskite-based phase. The heating at 500°C temperature improved the homogeneity of the run products and led to diffraction patterns with sharp peaks. Our experimental results at 500°C do not support a complete solid solution PdTe–PdBi. Kotulskite dissolves up to 40.3 at.% Bi, $Pd_{0.99}(Te_{0.21}Bi_{0.80})_{\Sigma 1.00}$ and at this maximum the solid solution breaks and there is a gap up to the composition $Pd_{1.00}(Bi_{0.96}Te_{0.04})_{\Sigma 1.00}$, which is the formation of PdBi dissolving 1.6 at.% Te (Fig. 3c and Fig. 4). Experiment no. KtBi45 (Fig 4, Table 3) clearly shows the presence of two phases $Pd_{0.99}(Te_{0.21}Bi_{0.80})_{\Sigma 1.00}$ + $Pd_{1.00}(Bi_{0.96}Te_{0.04})_{\Sigma 1.00}$. It is interesting to note that the experimental products with PdBi composition prepared at 400°C and 500°C show monoclinic structure with $P2_1$ space group described by Bhatt and Schubert (1979). This phase, also denoted as α-PdBi by Okamoto (1994), transforms at 210°C to an orthorhombic structure of β-PdBi (Zhuravlev, 1957). This transformation seems to be martensitic and the orthorhombic phase is not quenchable (Bhatt and Schubert, 1979). Sobolevskite was originally described by Evstigneeva *et al.* (1976) as hexagonal, isostructural with nickeline. However, its diffraction pattern contains nine additional reflections, which cannot be explained by the hexagonal NiAs structure-type, but nevertheless are consistent with the monoclinic $P2_1$ structure of α-PdBi (Bayliss, 1990). The exact symmetry of sobolevskite is not fully clear and requires further examination.

The unit-cell parameters of kotulskite solid solutions synthetised at 500°C are summarised in Table 4. Figure 2 shows the evolution of unit-cell volume. The incorporation of Bi into the kotulskite structure results in a significant increase of the unit-cell volume from 84.69 Å^3 to 87.29 Å^3. Bismuth substitutes for Te.

Copper solubility

Kotulskite dissolves up to 5.6 at.% Cu at 400°C. Kotulskite ss forms a stable association with merenskyite ($PdTe_2$) and Cu-telluride ss. The Cu for Pd substitution in the Cu-kotulskite solid solution results in a decrease of unit-cell volume from 84.69 to 82.57 Å^3.

Lead solubility

Kotulskite forms an extensive solid solution dissolving Pb, up to 30 at.% Pb (Vymazalová and Drábek, 2011) where it breaks because the PdTe structure cannot accommodate any more Pb.

https://doi.org/10.1180/mgm.2025.9 Published online by Cambridge University Press

Lead substitutes Te in the solid solution. The incorporation of Pb has a negligible impact on the unit cell volume, which remains approximately constant within the solid solution.

Antimony solubility

The solubility of Sb in kotulskite was confirmed up to the composition $Pd(Te_{0.18}Sb_{0.82})_{\Sigma 1.00}$, PdTe dissolving 41.1 at.% Sb, run no. KtSb40 (Table 3). The experiments at the compositional range $Pd(Te_{0.18}Sb_{0.82})_{\Sigma 1.00}$ – Pd(Sb,Te), runs KtSb43, KtSb45, KtSb47 (Table 2) are not conclusive. The products of these experiments, based on SEM and EPMA observations, seem to be inhomogeneous. Therefore, we cannot satisfactorily confirm a complete solid solution. Neither long-term heating (and the repetition of the same experiments) nor heating at higher temperature (450 and 500°C) improved the experimental products to be able to confirm the kotulskite-based hexagonal structure. Furthermore, heating at 500°C resulted in the appearance of a liquid phase in the system.

Kim and Chao (1991) at 600°C, and El-Boragy and Schubert (1971) at 400°C, reported a complete PdTe–PdSb solid solution. However, their study is based on powder X-ray diffraction phase analysis (i.e. no Rietveld refinement was performed) and hence the appearance of two nearly similar kotulskite-based phases might have been overlooked in their study.

Incorporation of Sb into the kotulskite structure, in the compositional range Sb from 4.7 to 40.1 at.% led to lowering of unit-cell volume from 84.69 to 81.85 Å^3, Fig. 2.

Tin solubility

Our experimental study confirmed the solubility of Sn in kotulskite, up to 20 at.% Sn, as suggested by Vymazalová and Drábek (2010). At this composition the solid solution breaks, the stable association $Pd_{20}Sn_{13}$ + ternary phase PdSnTe + kotulskite ss forms (Fig. 3d). The Sn for Te substitution results in a significant decrease of the unit-cell volume from 84.69 to 79.99 Å^3 (Fig. 2). It is interesting to note that vacancies occur on the Pd position in this solid solution as we detected a change in the Pd stoichiometry [i.e. from $Pd_{1.00}Te_{1.00}$ to $Pd_{0.93}(Te_{0.65}Sn_{0.42})_{\Sigma 1.07}$]. The introduction of vacancies on the Pd sites in the Sn-kotulskite solid solution very likely contributes to the lowering of the unit cell volume.

Conclusions

The solubility of selected elements in the synthetic analogue of kotulskite (PdTe) was investigated experimentally. The ranges of solid solutions in the systems Pd–Te–A, with A = Ag, As, Bi, Cu, Pb, Sb and Sn at 400°C (at 500°C for Bi) were constrained.

Kotulskite does not dissolve Ag. Kotulskite may dissolve up to 3 at.% As, up to 5.6 at.% Cu, up to 20 at.% Sn and up to 30 at.% Pb. Continuous complete solid solution between kotulskite – sudburyite and kotulskite – sobolevskite has not been confirmed within this study. The synthetic analogue of kotulskite dissolves up to 40 at.% Bi and at this composition $Pd_{0.99}(Te_{0.21}Bi_{0.80})_{\Sigma 1.01}$ the solid solution breaks and forms a gap up to the composition $Pd_{1.00}(Bi_{0.97}Te_{0.03})_{\Sigma 1.00}$. This observation was further supported by additional heating of experimental series at 500°C. The coexistence of $Pd_{0.99}(Te_{0.21}Bi_{0.80})_{\Sigma 1.01}$ and $Pd_{1.00}(Bi_{0.97}Te_{0.03})_{\Sigma 1.00}$ with their contrasting phase boundaries are clearly visible in back-scattered electron (BSE) images. The solid-solution series PdTe–PdSb are also limited, the synthetic analogue of kotulskite dissolves up to 41.1 at.% Sb and at this composition some inhomogeneity appears.

Copper substitutes for Pd whereas As, Bi, Pb, Sb and Sn substitute for Te in the crystal structure of kotulskite.

The assessed ranges of kotulskite solid-solution series at 400°C and the determination of the maximum solubility of selected elements, supported by EPMA and XRD data, may enhance the data interpretation observed in natural conditions. In particular, a misinterpretation of parts of the solid-solution series as potential and distinct new minerals. The end-members $Pd(Te_{0.2}Bi_{0.8})$, $Pd(Te_{0.4}Pb_{0.6})$, $Pd(Te_{0.2}Sb_{0.8})$ and $Pd(Te_{0.6}Sn_{0.4})$ of solid solutions found in nature and ternary compounds that do not fall in the solid solution field may represent potential new minerals. The results obtained present the end-members of selected solid solutions of kotulskite, incorporating As, Bi, Cu, Pb, Sb and Sn under the laboratory conditions at 400°C (500°C for Bi).

The established solid-solution series and proved stable associations can be found in Cu–Ni–PGE mineral deposits associated with mafic and ultramafic igneous rocks and probably exist at other types of deposits rich in PGE and Cu, Bi, Pb, Sb, Sn-enriched fluids.

The knowledge of solid-solution series in the systems studied may also be applied in mineral processing, in particular for the extraction of certain elements from the ore-concentrates.

Kotulskite crystalises in the NiAs structure type, which is very stable and a common structure for AB minerals/phases with chalcogen and a transition metal. The structure can adopt various substitutions by changing the unit-cell parameters. Also, a non-stoichiometry on metallic and chalcogen sites can occur to a certain extent, which makes the structure even more flexible and allows various minor elements to be accommodated. Kotulskite may play a role as the container of minor elements.

Acknowledgements. Constructive comments made by reviewers Louis J. Cabri, Nadhezda D. Tolstykh and an anonymous reviewer are greatly appreciated; they improved the quality of the manuscript. The editorial handling by Stuart Mills is also acknowledged. The authors are grateful to Z. Korbelová (Geological Institute of the Czech Academy of Sciences, v.v.i.) for performing the electron-microprobe analyses.

Financial Statement. Financial support through the Project No 22-26485S from the Czech Science Foundation (GACR) is gratefully acknowledged.

Competing interests. The authors declare none.

References

Arnason J.G., Bird D.K., Bernstein S. and Kelemen P.B. (1997) Gold and platinum-group element mineralization in the Kruuse Fjord gabbro complex, east Greenland. *Economic Geology*, **92**, 490–501.

Barkov A.Y., Laflamme J.H.G., Cabri L.J. and Martin R.F. (2002) Platinum-group minerals from the Wellgreen Ni–Cu–PGE deposit, Yukon, Canada. *The Canadian Mineralogist*, **40**, 651–669.

Barkov A.Y., Shvedov G.I., Polonyankin A.A., Martin R.F. and O'Driscoll B. (2017) New and unusual Pd–Tl-bearing mineralization in the Anomal'nyi deposit, Kondyor concentrically zoned complex, northern Khabarovskiy kray, Russia. *Mineralogical Magazine*, **81**, 679–688.

Barkov A.Y., Nikiforov A.A., Barkova L.P. and Martin R.F. (2022) Occurrences of Pd–Pt bismuthotellurides and a phosphohedyphane–like phase in sulfide veins of the Monchepluton layered complex, Kola Peninsula, Russia. *Minerals*, **12**, 624.

Barkov A.Y., Nikulin I.I., Nikiforov A.A., Lobastov B.M., Silyanov S.A. and Martin R.F. (2021) Atypical mineralization involving Pd–Pt, Au–Ag, REE, Y, Zr, Th, U, and Cl–F in the Oktyabrsky Deposit, Noril'sk Complex, Russia. *Minerals*, **11**, 1193.

Bayliss P. (1990) Revised unit–cell dimensions, space group, and chemical formula of some metallic minerals. *The Canadian Mineralogist*, **28**, 751–755.

https://doi.org/10.1180/mgm.2025.9 Published online by Cambridge University Press

Beaudoin G., Laurent R. and Ohnenstetter D. (1990) First report of platinum-group minerals at Blue lake Labrador Trough, Quebec. *The Canadian Mineralogist*, **28**, 409–418.

Bhatt Y.C. and Schubert K. (1979) Kristallstruktur von PdBi.r. *Journal of the Less-Common Metals*, **64**, 17–24.

Bruker A.X.S. (2014) *Topas 5, computing program*. Bruker AXS Gmbh, Karlrsuhe, Germany

Cabri L.J. (2002) The platinum-group minerals. Pp. 13–129 In: *The geology, mineralogy and mineral beneficiation of platinum-group elements* (Cabri, L.J., editor). Canadian Institute of Mining and Metallurgy, **Vol. 54**.

Cabri L.J. and Laflamme J.H.G. (1976) The mineralogy of the platinum-group elements from some copper–nickel deposits of the Sudbury area, Ontario. *Economic Geology*, **71**, 1159–1195.

Cabri L.J. and Laflamme J.H.G. (1979) Mineralogy of samples from Lac des Iles area, Ontario. *Canada Centre for Mineral and Energy Technology Report*, 79–29. pp19

Cabri L.J., Rowland J.F., Laflamme J.H.G. and Stewart J.M. (1979) Keithconnite, telluropalladinite and other Pd–Pt tellurides from the Stillwater Complex, Montana. *The Canadian Mineralogist*, **17**, 589–594.

Cabri L.J., Harris D.C. and Weiser T.W. (1996) The mineralogy and distribution of platinum-group mineral (PGM) placer deposits of the world. *Exploration and Mining Geology*, **5**, 73–167.

Cook N.J., Ciobanu C.L., Merkle R.K.W. and Bernhardt H.-J. (2002) Sobolevskite, taimyrite, and Pt_2CuFe (tulameenite?) in complex massive talnakhite ore, Talnakh Orefield, Russia. *The Canadian Mineralogist*, **40**, 329–340.

Criddle A.J. and Stanley C.J. (1993) *Quantitative Data File for Ore Minerals*, *3rd Edition*. Chapman and Hall, London, 635pp.

El-Boragy M. and Schubert K. (1971) Uber einige Varianten der NiAs-Familie in Mischungen des Palladiums mit B-Elementen. *Zeitschrift für Metallkunde*, **62**, 314–323.

El Ghorfi M., Oberthür T., Melcher, F., Lüders V., El Boukhari A., Maacha L., Ziadi R. and Baoutoul H. (2006) Gold–palladium mineralization at Bleïda Far West, Bou Azzer–El Graara Inlier, Anti–Atlas, Morocco. *Mineralium Deposita*, **41**, 549–564.

Evstigneeva, T.L., Genkin A.D. and Kovalenker V.A. (1976) Sobolevskite, a new bismuthide of palladium, and the nomenclature of minerals of the system PdBi–PdTe–PdSb. *International Geological Review*, **18**, 856–866. [Translation of Evstigneeva *et al.* (1975) *Zapiski Vsesoyuznogo Mineralogicheskogo Obshchestva*, **104**, 568–579].

Evstigneeva P.V., Nickolsky M.S., Geringer N.V., Vymazalová A., Nekrasov A.N. and Chareev D.A. (2019) Pt- and Pd-bismuthotellurides: phase relations in the Pt–Bi–Te and Pd–Bi–Te systems. *Proceedings of the 15th Biennial SGA Meeting*, 27–30 August 2019, Glasgow, UK.

Genkin A.D., Zhuravlev N.N. and Smirnova E.M. (1963) Moncheite and kotulskite – new minerals – and the composition of michenerite. *Zapiski Vsesoyuznogo Mineralogicheskogo Obshchestva*, **92**, 33–50. [in Russian]

Grokhovskaya, T.L., Distler, V.V., Klyunin, S.F., Zakharov, A.A. and Laputina, I.P. (1992) Low–sulfide platinum group mineralization of the Lukkulaisvaara pluton, northern Karelia. *International Geology Review*, **34**, 503–520.

Grokhovskaya T.L., Lapina M.I., Ganin V.A. and Grinevich N.G. (2005) PGE mineralization in the Burakovsk layered complex, southern Karelia, Russia. *Geology of Ore Deposits*, **47**, 283–308.

Gronvold F. and Rost E. (1956) On the sulfides, selenides and tellurides of palladium, *Acta Chemica Scandinavica*, **10**, 1620–1634.

Kingston G.A. (1966) The occurrence of platinoid bismuthotellurides in the Merensky Reef at Rustenburg platinum mine in the western Bushveld. *Mineralogical Magazine*, **35**, 815–835.

Konnikov E.G., Orsoev D.A., Veselovskii N.N. and Glotov A.I. (1993) Distribution of platinum group elements in the "Ore bed of Sopcha" of the Monchegorsk layered pluton. *Russian Geology and Geophysics*, **34**, 98–104.

Kovalenker V.A., Laputina I.P., Vyal'sov L.N., Genkin A.D. and Evstigneeva T.L. (1973) Tellurium minerals in copper–nickel sulfide ores at Talnakh and Oktyabr (Noril'sk district). *International Geology Review*, **15**, 1284–1294.

Lavrov O.B. and Kuleshevich LV. (2017) Platinoids in the Kaalamo Differentiated Massif in the Northern Ladoga Region, Karelia, Russia. *Geology of Ore Deposits*, **59**, 632–641.

Mulja T. and Mitchell R.H. (1991) The Geordie Lake Intrusion, Coldwell Complex, Ontario; a palladium–and tellurium–rich disseminated sulfide occurrence derived from an evolved tholeiitic magma. *Economic Geology*, **86**, 1050–1069.

Okamoto H. (1994) The Bi-Pd (Bismuth-Palladium) system. *Journal of phase equilibria*, **15**, 191–194.

PANalytical, B.V. (2012) *HighScore 3.0*. Almelo, The Netherlands.

Shaybekov R.I., Makeev B.A., Kononkova N.N., Isaenko S.I. and Tropnikov E.M. (2021) Palladium tellurides and bismuthtellurides in sulfide copper–nickel ores of the Savabeisky ore occurrence (Nenets Autonomous District, Russia). *Lithosphere*, **21**, 574–594.

Sluzhenikin S.F. (2011) Platinum–copper–nickel and platinum ores of Noril'sk region and their ore mineralization. *Russian Journal of General Chemistry*, **81**, 1288–1301.

Spiridonov E.M., Orsoev D.A., Ariskin A.A., Nikolaev G.S., Kislov E.V., Korotaeva N.N. and Yapaskurt V.O. (2019) Hg- and Cd-bearing Pd, Pt, Au, and Ag minerals in sulfide–bearing mafic and ultramafic rocks of the Yoko–Dovyren intrusion in the Baikalides of the northern Baikal area. *Geochemistry International*, **57**, 42–55.

Spiridonov E.M., Belyakov S.N., Korotaeva N.N., Egorov K.V., Ivanova Y.A., Naumov D.I. and Serova A.A. (2020) Menshikovite $Pd_3Ni_2As_3$ and associating minerals of sulfide ores at the eastern flank of the Oktyabrsky deposit (Noril'sk Ore Field). *Moscow University Geology Bulletin*, **75**, 472–480.

Tolstykh N.D. (2008) PGE mineralization in marginal sulfide ores of the Chineisky layered intrusion, Russia. *Mineralogy and Petrology*, **92**, 283–306.

Tolstykh N.D., Zhitova L.M., Shapovalova M.O. and Chayka I.F. (2019) The evolution of the ore–forming system in the low sulfide horizon of the Noril'sk 1 intrusion, Russia. *Mineralogical Magazine*, **83**, 673–694.

Vymazalová A. and Drábek M. (2010) The system Pd–Sn–Te at 400°C and mineralogical implications. II. The ternary phases. *The Canadian Mineralogist*, **48**, 1051–1058.

Vymazalová A. and Drábek M. (2011) The Pd–Pb–Te system: phase relations involving pašavaite and potential minerals. *The Canadian Mineralogist*, **49**, 1679–1686.

Vymazalová A., Laufek F., Kristavchuk A.V., Chareev D.A. and Drábek M. (2015) The system Ag–Pd–Te: phase relations and mineral assemblages. *Mineralogical Magazine*, **79**, 1813–1832.

Kim W–S. and Chao G.Y. (1991) Phase relations in the system Pd–Sb–Te. *The Canadian Mineralogist*, **29**, 401–409.

Watkinson D.H. and Ohnenstetter D. (1992) Hydrothermal origin of platinum-group mineralization in the Two Duck Lake intrusion, Coldwell Complex, northwestern Ontario. *The Canadian Mineralogist*, **30**, 121–136.

Yushko-Zakharova O.Y., Avdonin A.S., Bykov V.P., Kulagov Ye A., Lebedeva S.I., Chernyayev L.A. and Yurkina K.V. (1972). Composition of platinum minerals in copper–nickel ores of the Talnakh and Noril'sk deposits. *Mineralogical Studies, 2nd Edition*. Moscow: IMGRE.

Zagorac D., Müller H., Ruehl S., Zagorac J. and Rehme S.J. (2019) Recent developments in the Inorganic Crystal Structure Database: theoretical crystal structure data and related features. *Journal of Applied Crystallography*, **52**, 918–925.

Zhuravlev N.N. (1957) Structure of superconductors. X. Thermal, microscopic and X-ray investigation of the bismuth–palladium system. *Zhurnal Eksperimental'noi i Teoreticheskoi Fiziki*, **5**, 1064–1072.

https://doi.org/10.1180/mgm.2025.9 Published online by Cambridge University Press